Available online at www.sciencedirect.com
SCIENCE DIRECT®
Journal of Organometallic Chemistry 664 (2002) 94–105
Journal of Organometallic Chemistry
www.elsevier.com/locate/jorganchem

Stepwise assembly and structural characterization of oligonuclear ferrocene aggregates with boron–nitrogen backbone

Kuangbiao Ma [a], Hans-Wolfram Lerner [a], Stefan Scholz [a], Jan W. Bats [b], Michael Bolte [b], Matthias Wagner [a,*]

[a] Institut für Anorganische Chemie, J.W. Goethe-Universität Frankfurt, Marie-Curie-Strasse 11, D-60439 Frankfurt (Main), Germany
[b] Institut für Organische Chemie, J.W. Goethe-Universität Frankfurt, Marie-Curie-Strasse 11, D-60439 Frankfurt (Main), Germany

Received 4 July 2002; accepted 9 September 2002

Abstract

The reaction of $FcBBr_2$ [**1**; $Fc = (C_5H_5)Fe(C_5H_4)$] with either 4-bromo-*N*,*N*-bis(trimethylsilyl)aniline or lithium *N*-*tert*-butyltrimethylsilylamide or sodium *N*,*N*-bis(trimethylsilyl)amide or 4-methoxyaniline in the appropriate stoichiometric ratio yields mononuclear {$FcB(Br)N(SiMe_3)(C_6H_4Br)$ (**3**); $FcB(Br)N(SiMe_3)(CMe_3)$ (**4**)}, dinuclear {$[FcB(Br)]_2NSiMe_3$ (**5**); $[FcBN(H)(C_6H_4OMe)]_2NC_6H_4OMe$ (**6**)}, trinuclear {$[FcBN(C_6H_4OMe)]_3$ (**7**)} and tetranuclear {$[FcB(Br)N(SiMe_3)FcB]_2NH$ (**8**)} ferrocene complexes, which are held together by covalent boron–nitrogen bonds. All compounds **3**–**8** have been characterized by X-ray crystallography. Compound **7** features a puckered borazine core, while the BN backbone of **8** adopts a helical conformation. Treatment of 1,1′-$fc(BBr_2)_2$ [**10**; $fc = (C_5H_4)_2Fe$] with 4-bromo-*N*,*N*-bis(trimethylsilyl)aniline produces the 1,3-dibora-[3]ferrocenophane **13**, in which a $-B(Br)N(C_6H_4Br)B(Br)-$ bridge spans both cyclopentadienyl rings. Polymeric byproducts have not been observed. These results indicate a strong preference for the formation of *intra*molecular BNB *ansa*-bridges over *inter*molecular BNB crosslinks.

Keywords: Oligonuclear ferrocene complexes; Boron–nitrogen backbone; X-ray crystallography

1. Introduction

Oligonuclear aggregates of organometallic compounds are currently attracting growing attention. Useful applications can be anticipated in the fields of magnetic, electronic and liquid crystalline materials [1–4]. In this context, a variety of systems containing two or more ferrocenyl moieties have been synthesized to investigate the efficiency of different bridging units as transmitters of electronic interactions [5]. For example, in 1,3,5-triferrocenylbenzene only negligible electronic communication between the ferrocenyl groups is observed, whereas a strong correlation between the redox-active termini has been reported for 2,5-diferrocenylthiophene [6].

Boroxine, $H_3B_3O_3$, and borazine, $H_6B_3N_3$, are inorganic analogues of benzene. Both compounds are planar and possess a π system of six electrons. The degree of electron delocalization in boroxine and borazine is still a subject of some debate, but at least the latter compound appears to have some aromatic character, even though the aromatic stabilization is much weaker than that of benzene itself [7,8]. These results prompted us to exploit the facile formation of boron–oxygen- and boron–nitrogen bonds for the synthesis of oligonuclear ferrocenylarene analogues in which the organic core is replaced by the isoelectronic inorganic heterocycles. The general route to triorganoboroxines [9] and tri- or hexaorganoborazines [10] is known for a long time [11], however, only few derivatives bearing pendent redox-active organometallic substituents at boron have been reported up to now [e.g. $Fc_3B_3O_3$ [12], $Fc_3B_3(NH)_3$ [13]; $Fc = (C_5H_5)Fe(C_5H_4)$]. Recently, our group reported on the X-ray crystal structure determination of triferrocenylboroxine and triferrocenylborazine [14].

* Corresponding author. Fax: +49-69-79829260
E-mail address: matthias.wagner@chemie.uni-frankfurt.de (M. Wagner).

0022-328X/02/$ - see front matter
PII: S0022-328X(02)01968-X

The purpose of the work described in this paper was to synthesize and isolate open-chain intermediates of the borazine assembly in order: (i) to get insight into the reaction mechanism and to compare their structural characteristics with those of the final heterocyclic product; (ii) to find ways for the generation of mixed borazines $Fc_xMc_yB_3(NR)_3$ ($x = 1, 2$; $y = 3-x$) bearing organometallic substituents Mc other than ferrocenyl at selected boron atoms. Moreover, we wanted to explore whether ferrocene-containing polymers with boron–nitrogen backbone can be synthesized starting from 1,1′-diborylferrocene and appropriate amine reagents.

2. Results and discussion

2.1. Syntheses

Treatment of $FcBBr_2$ (**1**) with one equivalent of hexamethyldisilazane in toluene at 50 °C gave the parent triferrocenylborazine (**2**) in high yield (Scheme 1).

This compound, which had already been synthesized earlier by Kotz and Painter using a different procedure [13], was re-investigated here to gather information about the optimum access route. The amino(bromo)borylferrocene complexes **3** and **4** were generated from **1**, 4-bromo-*N*,*N*-bis(trimethylsilyl)aniline (hexane, ambient temperature) and lithium *N*-*tert*-butyltrimethylsilylamide (hexane/toluene, ambient temperature), respectively (Scheme 2). In a similar reaction, **1** and sodium *N*,*N*-bis(trimethylsilyl)amide (NaNSi; molar ratio 2:1; heptane/toluene, ambient temperature) gave the dinuclear species **5**. Further intermediates of the stepwise triferrocenylborazine assembly were available from the controlled aminolysis of $FcBBr_2$ (**1**) in the presence of

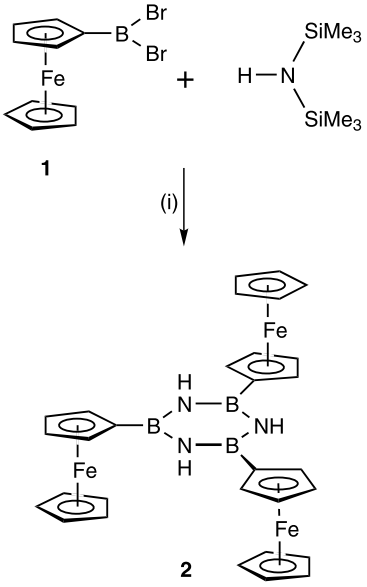

Scheme 1. (i) In toluene, 0–50 °C.

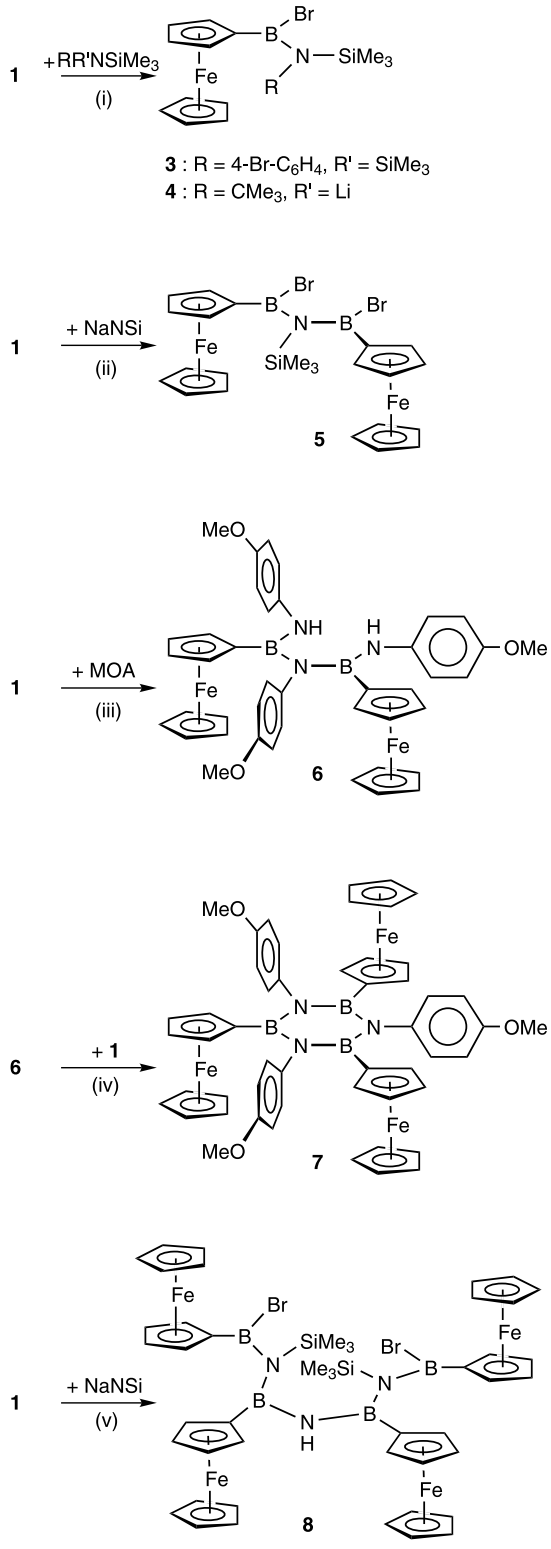

Scheme 2. (i) Compound **3**: in hexane, ambient temperature. **4**: in toluene–hexane, 0 °C to ambient temperature; (ii) in toluene–heptane, −78 °C to ambient temperature, NaNSi = $NaN(SiMe_3)_2$; (iii) $+Et_3N$, in toluene, −78 °C to ambient temperature, MOA = 4-methoxyaniline; (iv) *method 1:* $+Et_3N$, in toluene, −78 °C to reflux temperature; *method 2:* +n-BuLi, in toluene, −78 °C to ambient temperature; (v) in C_6D_6, ambient temperature, NaNSi = $NaN(SiMe_3)_2$.

NEt_3. This reaction, which worked best with amines combining high basicity with moderate steric bulk [e.g. 4-methoxyaniline (MOA)], led to the formation of the diferrocenyl derivative **6** (toluene, ambient temperature). Treatment of **6** with $FcBBr_2$ (**1**) resulted in the desired ring-closure reaction and gave the borazine **7** in very good yield (Scheme 2). This synthesis approach is likely to provide access also to mixed borazines $Fc_xMc_yB_3(NR)_3$ ($x = 1, 2$; $y = 3-x$) when borylated metallocenes $McBBr_2$ other than ferrocene are employed.

Few crystals of a tetranuclear aggregate **8** (Scheme 2) were obtained from the reaction of **1** and sodium *N*,*N*-bis(trimethylsilyl)amide (molar ratio 1:1; C_6D_6, ambient temperature), indicating, that the reaction mixture was contaminated by trace amounts of $HN(SiMe_3)_2$.

We have not been able to generate the boroxine **9** (Scheme 3) by hydrolysis of $FcBBr_2$ (**1**), but always observed the formation of free ferrocene. Treatment of $FcB(NMe_2)_2$ with water gives a rather stable dimethylamine adduct of **9**, which is difficult to transform into an analytically pure sample of the free boroxine. In contrast, **9** can be conveniently prepared by the hydrolysis of the open-chain compound **6** or the borazine **7**.

Attempts to synthesize ferrocene-containing polymers or three-dimensional networks employing the boron–nitrogen chemistry developed in this chapter revealed fundamental problems already at an early stage: treatment of 1,1′-fc$(BBr_2)_2$ [**10**; fc = $(C_5H_4)_2Fe$] with one or two equivalents of 4-bromo-*N*,*N*-bis(trimethylsilyl)aniline at ambient temperature gave the open-chain complexes **11** or **12**, respectively (Scheme 4).

Heating of **11** in toluene to reflux temperature afforded the ferrocenophane **13** rather than an oligonuclear aggregate (Scheme 4; related 1,3-dibora-[3]ferrocenophanes have already been described by Wrackmeyer and Herberhold [15]). Toluene solutions of the 1,1′-disubstituted derivative **12** were found to be thermally more stable. However, in the presence of one

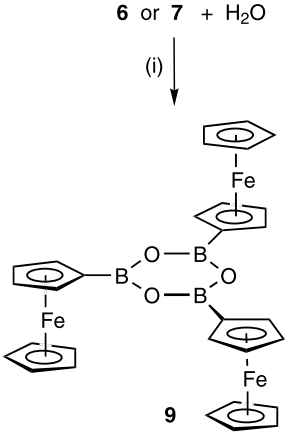

Scheme 3. (i) In toluene, ambient temperature.

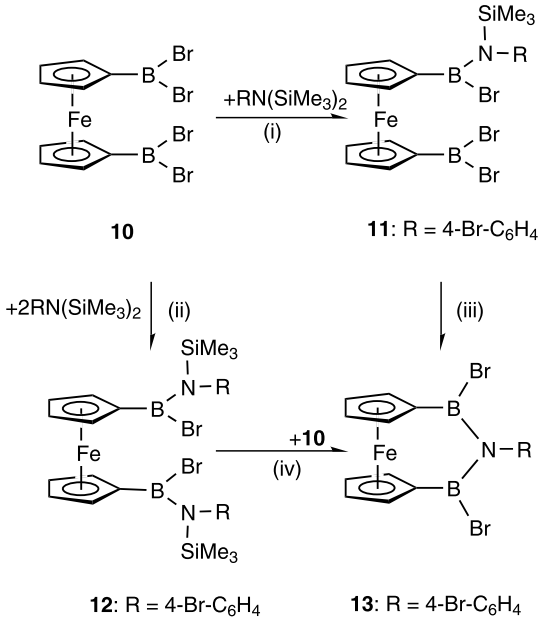

Scheme 4. (i) In toluene, −78 °C to ambient temperature; (ii) in toluene, ambient temperature; (iii) in toluene, reflux temperature; (iv) in toluene, −78 °C to reflux temperature.

equivalent of 1,1′-fc$(BBr_2)_2$ **10**, complex **13** was again generated in excellent yield. These results indicate a strong preference for the formation of *intra*molecular BNB *ansa*-bridges over *inter*molecular BNB crosslinks.

2.2. NMR spectroscopy

The ^{11}B-NMR resonances of all compounds under investigation here appear in the range between 30.9 (**3**) and 45.7 ppm (**4**), which is characteristic of three-coordinate boron centers bearing at least one π-electron donating substituent [16].

^{1}H- and ^{13}C-NMR spectroscopy on **3** and **4** at room temperature in C_6D_6–$CDCl_3$ solution revealed one set of signals only. The ^{1}H-NMR spectrum of **3** does not change at elevated temperature (100 °C; toluene-d_8); at $T = -70$ °C, however, the signals of the substituted cyclopentadienyl ring become extremely broad. Consequently, rotation about the B–N bond appears to be fast on the NMR time scale at ambient temperature thereby testifying to a comparatively low degree of B–N π-bonding.

The integral values in the ^{1}H-NMR spectra of **2**–**7** and **11**–**12** are in accord with the molecular structures proposed in Schemes 1, 2 and 4 (due to the very low yield, decent NMR spectra of **8** were not obtained; ^{11}B-, ^{1}H- and ^{13}C-NMR shift values of the boroxine **9** have been reported previously [12,14]). Most proton and carbon resonances appear in the usually observed ranges and thus do not merit further discussion. One remarkable exception is provided by the ^{1}H-NMR signals of the substituted cyclopentadienyl rings in the borazine **7**,

which appear at $\delta(^1H, CDCl_3) = 2.87$ and 4.00. The pronounced upfield shift of the former resonance is most likely due to the magnetic anisotropy effect of the neighboring 4-methoxyphenyl rings. This feature is absent in the proton NMR spectrum of the more flexible open-chain compound **6** and therefore gives further evidence for the assumption that **7** possesses a rigid cyclic core, which suffers from severe steric congestion.

The ^{11}B-NMR signal of the *ansa*-ferrocene **13** is found at $\delta(^{11}B; CDCl_3) = 40.0$. Compared to the starting material 1,1′-fc$(BBr_2)_2$ **10** [$\delta(^{11}B; C_6D_6) = 50.3$] [17] the signal is shifted to higher field by 10.3 ppm. Compared to the borylamine 1,1′-fc[B(Br)pyr]$_2$ [$\delta(^{11}B; CDCl_3) = 34.4$; Hpyr = pyrrolidine] [18], it is less shielded by 5.6 ppm. The ^{11}B-NMR spectrum recorded for **13** is thus in agreement with the proposed diborylamine structure. The integrals in the ^1H-NMR spectrum of **13** reveal a 1:1 ratio between the ferrocenyl backbone (two resonances) and the 4-bromophenyl substituent (two resonances).

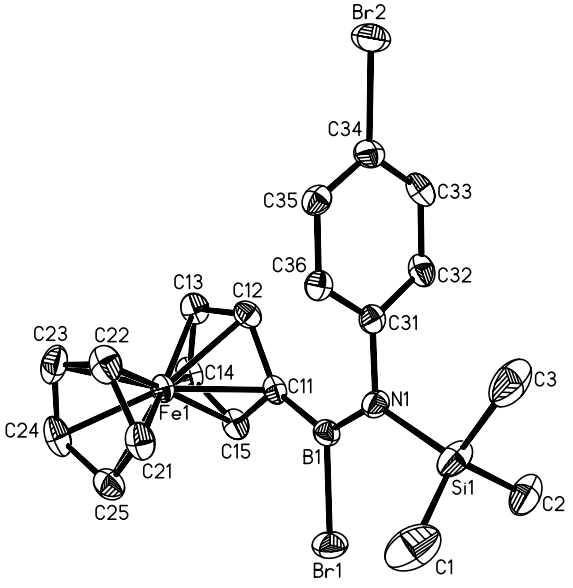

Fig. 1. Molecular structure and numbering scheme of compound **3** with hydrogen atoms omitted for clarity. Thermal ellipsoids are shown at the 50% probability level. Selected bond lengths (Å), angles (°) and torsion angles (°) of **3**: B(1)–N(1) = 1.404(3), B(1)–C(11) = 1.543(3), B(1)–Br(1) = 1.983(2), N(1)–C(31) = 1.443(3), N(1)–Si(1) = 1.797(2); C(11)–B(1)–N(1) = 129.6(2), N(1)–B(1)–Br(1) = 116.0(2), B(1)–N(1)–Si(1) = 127.5(2), B(1)–N(1)–C(31) = 117.2(2); C(12)–C(11)–B(1)–N(1) = −15.4(4), C(12)–C(11)–B(1)–Br(1) = 166.4(2), C(11)–B(1)–N(1)–C(31) = 4.0(3), C(11)–B(1)–N(1)–Si(1) = −169.0(2), Br(1)–B(1)–N(1)–C(31) = −177.8(1), Br(1)–B(1)–N(1)–Si(1) = 9.2(2), B(1)–N(1)–C(31)–C(32) = −90.8(2), B(1)–N(1)–C(31)–C(36) = 90.5 (2).

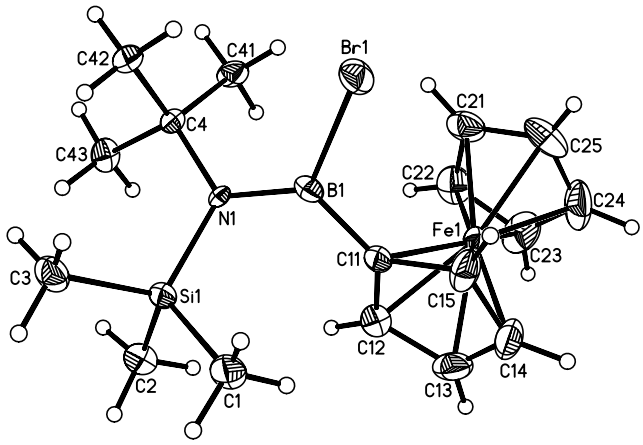

Fig. 2. Molecular structure and numbering scheme of compound **4**. Thermal ellipsoids are shown at the 50% probability level. Selected bond lengths (Å), angles (°) and torsion angles (°) of **4**: B(1)–N(1) = 1.434(7), B(1)–C(11) = 1.518(9), B(1)–Br(1) = 2.003(6), N(1)–C(4) = 1.517(6), N(1)–Si(1) = 1.772(4); C(11)–B(1)–Br(1) = 113.2(4), C(11)–B(1)–N(1) = 125.1(5), N(1)–B(1)–Br(1) = 121.6(4), B(1)–N(1)–Si(1) = 116.5(3), B(1)–N(1)–C(4) = 121.2(4); C(12)–C(11)–B(1)–N(1) = 27.2(8), C(12)–C(11)–B(1)–Br(1) = −154.4(4), C(11)–B(1)–N(1)–C(4) = −142.6(5), C(11)–B(1)–N(1)–Si(1) = 48.1(6), Br(1)–B(1)–N(1)–C(4) = 39.1(6), Br(1)–B(1)–N(1)–Si(1) = −130.2(3).

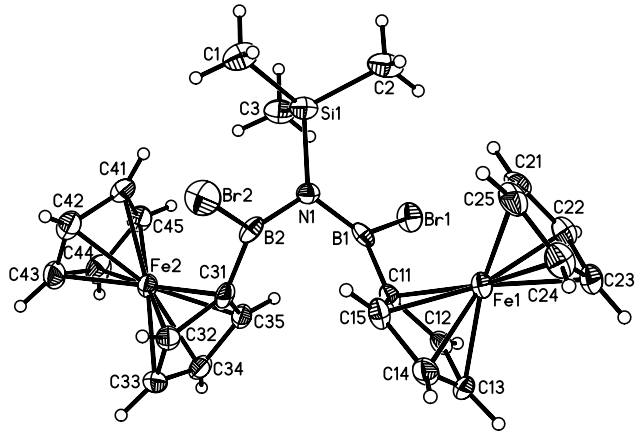

Fig. 3. Molecular structure and numbering scheme of compound **5**. Thermal ellipsoids are shown at the 50% probability level. Selected bond lengths (Å) angles (°) and torsion angles (°) of **5**: B(1)–N(1) = 1.426(6), B(2)–N(1) = 1.447(6), B(1)–C(11) = 1.530(7), B(2)–C(31) = 1.526(7), B(1)–Br(1) = 1.979(5), B(2)–Br(2) = 1.965(5), N(1)–Si(1) = 1.804(4); N(1)–B(1)–C(11) = 125.4(4), N(1)–B(2)–C(31) = 123.0(4), B(1)–N(1)–Si(1) = 121.7(3), B(2)–N(1)–Si(1) = 123.6(3), B(1)–N(1)–B(2) = 114.0(4), C(11)–B(1)–Br(1) = 114.2(3), C(31)–B(2)–Br(2) = 115.7(3); Si(1)–N(1)–B(1)–C(11) = 152.2(3), Si(1)–N(1)–B(2)–C(31) = 124.2(4), Si(1)–N(1)–B(1)–Br(1) = −28.5(5), Si(1)–N(1)–B(2)–Br(2) = −59.2(5), C(11)–B(1)–N(1)–B(2) = −37.1(6), C(31)–B(2)–N(1)–B(1) = −46.2(6), Br(1)–B(1)–N(1)–B(2) = 142.1(3), Br(2)–B(2)–N(1)–B(1) = 130.3(4).

2.3. X-ray crystallography

The compounds **3**–**8** and **13** have been structurally characterized by X-ray crystallography (Figs. 1–7; crystallographic data are summarized in Table 1).

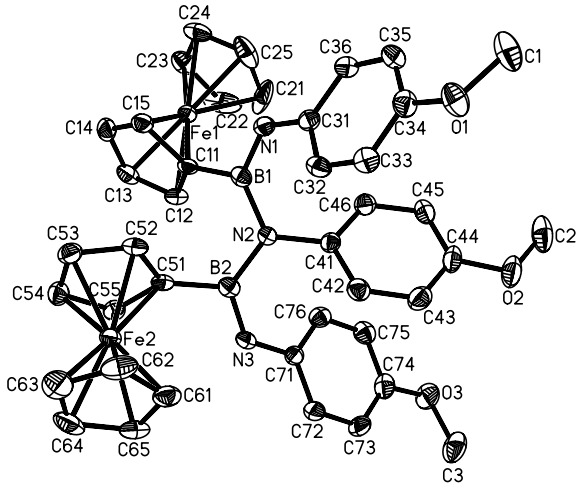

Fig. 4. Molecular structure and numbering scheme of compound **6** with hydrogen atoms omitted for clarity. Thermal ellipsoids are shown at the 50% probability level. Selected bond lengths (Å), angles (°) and torsion angles (°) of **6**: B(1)–N(1) = 1.423(3), B(1)–N(2) = 1.464(3), B(2)–N(2) = 1.458(3), B(2)–N(3) = 1.421(3), B(1)–C(11) = 1.556(4), B(2)–C(51) = 1.562(4), N(1)–C(31) = 1.408(3), N(2)–C(41) = 1.438(3), N(3)–C(71) = 1.418(3); B(1)–N(2)–B(2) = 119.3(2), N(1)–B(1)–N(2) = 123.3(2), N(2)–B(2)–N(3) = 125.1(2), N(1)–B(1)–C(11) = 117.6(2), N(2)–B(1)–C(11) = 119.0(2), B(1)–N(2)–C(41) = 119.7(2), B(2)–N(2)–C(41) = 120.8(2), N(3)–B(2)–C(51) = 116.9(2), N(2)–B(2)–C(51) = 117.9(2); N(1)–B(1)–N(2)–B(2) = 147.3(2), B(1)–N(2)–B(2)–N(3) = 150.3(2), C(11)–B(1)–N(1)–C(31) = 169.9(2), C(11)–B(1)–N(2)–C(41) = 141.1(2), B(1)–N(1)–C(31)–C(32) = −32.1(4), B(1)–N(2)–C(41)–C(42) = 144.8(2), C(51)–B(2)–N(2)–C(41) = 156.4(2), C(51)–B(2)–N(3)–C(71) = 166.7(2), B(2)–N(3)–C(71)–C(72) = 147.5(3).

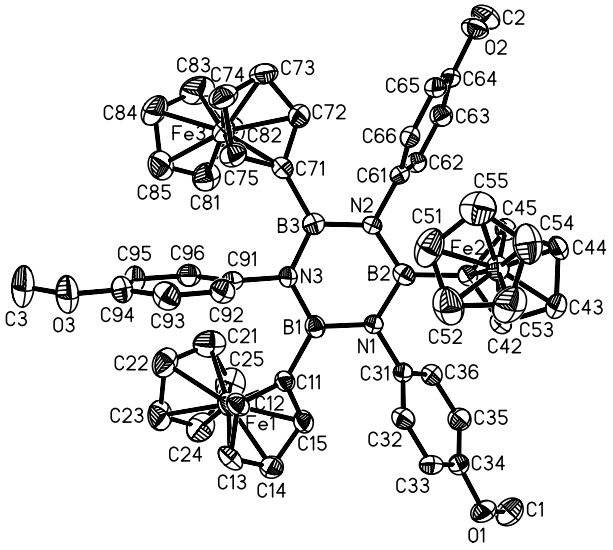

Fig. 5. Molecular structure and numbering scheme of the compound **7** with hydrogen atoms and solvent molecules omitted for clarity. Thermal ellipsoids are shown at the 50% probability level. Selected bond lengths (Å), angles (°) and torsion angles (°) of **7**: B(1)–N(1) = 1.454(5), B(1)–N(3) = 1.453(5), B(2)–N(1) = 1.456(5), B(2)–N(2) = 1.453(5), B(3)–N(2) = 1.456(5), B(3)–N(3) = 1.455(5), B(1)–C(11) = 1.582(5), B(2)–C(41) = 1.579(5), B(3)–C(71) = 1.579(5); B(1)–N(1)–B(2) = 122.2(3), B(1)–N(3)–B(3) = 122.7(3), B(2)–N(2)–B(3) = 123.2(3), N(1)–B(1)–N(3) = 116.2(3), N(1)–B(2)–N(2) = 115.4(3), N(2)–B(3)–N(3) = 114.9(3), C(11)–B(1)–N(1) = 119.9(3), C(11)–B(1)–N(3) = 123.8(3), C(31)–N(1)–B(1) = 119.4(3), C(31)–N(1)–B(2) = 118.3(3), C(41)–B(2)–N(1) = 121.3(3), C(41)–B(2)–N(2) = 123.2(3), C(61)–N(2)–B(2) = 118.3(3), C(61)–N(2)–B(3) = 118.3(3), C(71)–B(3)–N(2) = 120.9(3), C(71)–B(3)–N(3) = 124.0(3), C(91)–N(3)–B(1) = 117.9(3), C(91)–N(3)–B(3) = 119.4(3); B(1)–N(1)–B(2)–N(2) = −16.6(5), N(1)–B(2)–N(2)–B(3) = 21.5(5), B(2)–N(2)–B(3)–N(3) = −6.1(5), B(1)–N(3)–B(3)–N(2) = −15.6(5), N(1)–B(1)–N(3)–B(3) = 20.0(5), B(2)–N(1)–B(1)–N(3) = −2.9(5), N(1)–B(1)–C(11)–C(12) = 141.4(4), N(3)–B(1)–C(11)–C(12) = −35.8(6), B(1)–N(1)–C(31)–C(32) = −61.4(4), B(2)–N(1)–C(31)–C(32) = 115.2(4), N(1)–B(2)–C(41)–C(42) = −15.3(6), N(2)–B(2)–C(41)–C(42) = 161.3(3), B(2)–N(2)–C(61)–C(62) = 78.0(4), B(3)–N(2)–C(61)–C(62) = −106.9(4), N(2)–B(3)–C(71)–C(72) = 24.5(6), N(3)–B(3)–C(71)–C(72) = −160.0(3), B(1)–N(3)–C(91)–C(92) = 86.1(4), B(3)–N(3)–C(91)–C(92) = −93.5(4).

In the mononuclear complex **3** (space group $P2_1/c$; Fig. 1), the planar conformation of the B–N bond [torsion angles: C(11)–B(1)–N(1)–C(31) = 4.0(3), C(11)–B(1)–N(1)–Si(1) = −169.0(2)°], together with its length of only 1.404(3) Å indicate some double bond character as a result of N–B π-donation. The ferrocenyl and the 4-bromophenyl group on one hand and the bromo and trimethylsilyl substituent on the other adopt a *cis* configuration with respect to the B–N bond, thereby minimizing the steric congestion within the molecule. For the same reason, the 4-bromophenyl ring is rotated in a position orthogonal to the plane defined by the atoms B(1), N(1) and Si(1) [torsion angle: B(1)–N(1)–C(31)–C(32) = −90.8(2)°]. There is obviously no significant π interaction between the nitrogen atom and its 4-bromophenyl substituent in the solid state. A weak intramolecular C–H···π interaction exists between the C(12)–H(12) bond and the phenyl ring (distance H(12)···Cg = 2.71 Å, angle C(12)–H(12)–Cg = 143°; Cg: centroid of the phenyl ring).

The second monoferrocenyl complex **4** ($Pna2_1$; Fig. 2) bears a bulky *tert*-butyl group in addition to the trimethylsilyl substituent at the nitrogen atom. The molecular structure of **4** thus differs from that of the related complex **3** in a characteristic way: The B(1)–N(1) bond is no longer surrounded in a planar fashion by its substituents [torsion angles: C(11)–B(1)–N(1)–C(4) = −142.6(5), C(11)–B(1)–N(1)–Si(1) = 48.1(6)°], and it is elongated by 0.030 Å to a value of 1.434(7) Å. Moreover, the ferrocenyl substituent now comes close to the trimethylsilyl group, while the sterically more demanding *tert*-butyl substituent occupies the same side of the boron–nitrogen bond as the bromine atom.

The diborylamine **5** ($P2_1/n$; Fig. 3) features two different B–N bond lengths of B(1)–N(1) = 1.426(6) and B(2)–N(1) = 1.447(6) Å. The latter is longer than the boron–nitrogen link in the sterically less congested monoborylamine **3**. This can be explained by taking into account: (i) that the π-electron density supplied from the nitrogen lone pair has to be divided between two boron

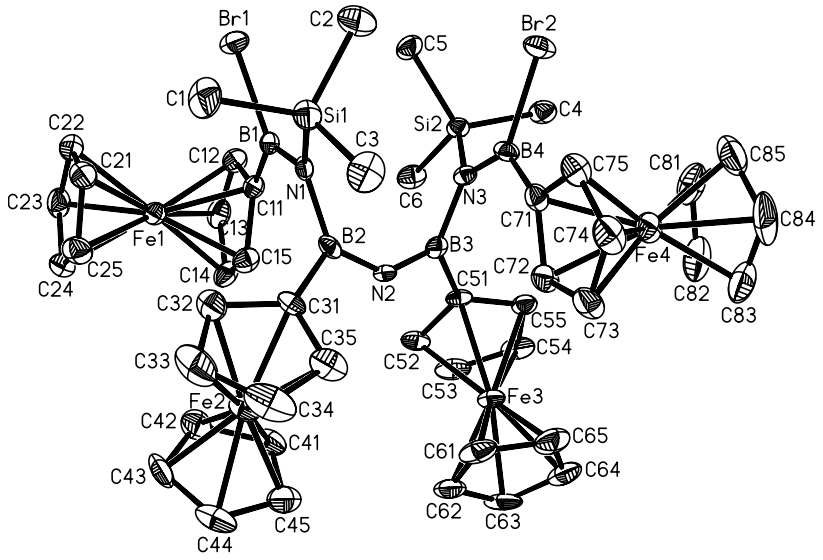

Fig. 6. Molecular structure and numbering scheme of compound **8** with hydrogen atoms and solvent molecules omitted for clarity. Thermal ellipsoids are shown at the 50% probability level. Selected bond lengths (Å), angles (°) and torsion angles (°) for **8**: B(1)–N(1) = 1.408(6), B(2)–N(1) = 1.495(6), B(2)–N(2) = 1.421(6), B(3)–N(2) = 1.443(6), B(3)–N(3) = 1.473(6), B(4)–N(3) = 1.411(6), B(1)–Br(1) = 1.982(5), B(4)–Br(2) = 1.994(5), B(1)–C(11) = 1.546(7), B(2)–C(31) = 1.561(7), B(3)–C(51) = 1.565(7), B(4)–C(71) = 1.532(7); B(1)–N(1)–B(2) = 119.5(4), B(2)–N(2)–B(3) = 140.4(4), B(3)–N(3)–B(4) = 118.8(4), N(1)–B(2)–N(2) = 123.4(4), N(2)–B(3)–N(3) = 122.2(4); B(1)–N(1)–B(2)–N(2) = 66.0(6), N(1)–B(2)–N(2)–B(3) = 11.4(9), B(2)–N(2)–B(3)–N(3) = 22.0(8), N(2)–B(3)–N(3)–B(4) = 62.0(6), C(11)–B(1)–N(1)–B(2) = 1.4(7), B(1)–N(1)–B(2)–C(31) = −113.9(5), B(3)–N(2)–B(2)–C(31) = −168.7(5), B(2)–N(2)–B(3)–C(51) = −157.7(5), B(4)–N(3)–B(3)–C(51) = −118.3(5), B(3)–N(3)–B(4)–C(71) = 9.0(7), Si(1)–N(1)–B(1)–Br(1) = 10.3(5), Si(2)–N(3)–B(4)–Br(2) = 14.7(5).

atoms in **5**, which in turn leads to a decrease of the individual B–N bond orders; and (ii) that the Br–B–N–Si torsion angles deviate considerably from the ideal value of 0°. The smaller angle possesses a value of Si(1)–N(1)–B(1)–Br(1) = −28.5(5)° and corresponds to the shorter boron–nitrogen bond, while the bigger one amounts to Si(1)–N(1)–B(2)–Br(2) = −59.2(5)° and corresponds to the longer B–N bond.

In the dinuclear complex **6** ($P2_1/c$; Fig. 4), the terminal B–N bonds are shorter [B(1)–N(1) = 1.423(3), B(2)–N(3) = 1.421(3) Å] and less twisted [C(11)–B(1)–N(1)–C(31) = 169.9(2), C(51)–B(2)–N(3)–C(71) = 166.7(2)°] than the internal B–N bonds [B(1)–N(2) = 1.464(3), B(2)–N(2) = 1.458(3) Å; C(11)–B(1)–N(2)–C(41) = 141.1(2), C(51)–B(2)–N(2)–C(41) = 156.4(2)°], which is in accord with the observa-

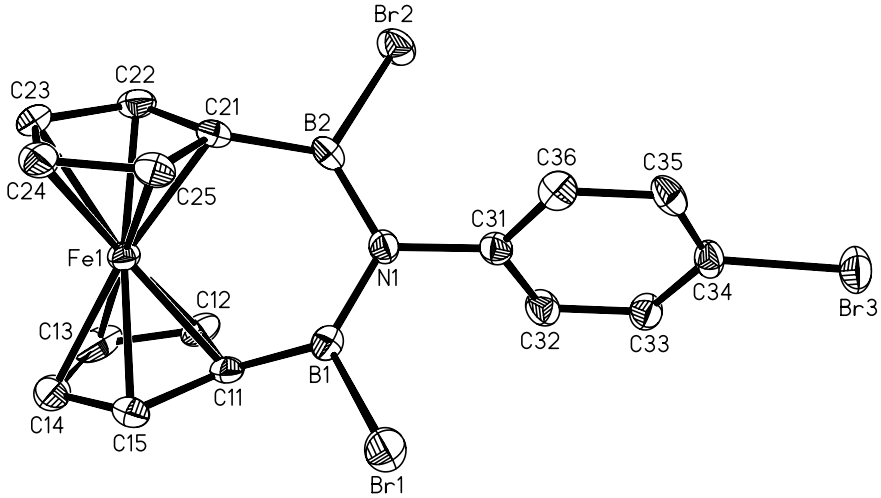

Fig. 7. Molecular structure and numbering scheme of compound **13** with hydrogen atoms omitted for clarity. Thermal ellipsoids are shown at the 50% probability level. Selected bond lengths (Å), angles (°), torsion angles and dihedral angles (°) for **13**: B(1)–N(1) = 1.448(5), B(2)–N(1) = 1.431(4), B(1)–Br(1) = 1.947(4), B(2)–Br(2) = 1.951(3), B(1)–C(11) = 1.531(5), B(2)–C(21) = 1.528(4), N(1)–C(31) = 1.449(4), Br(3)–C(34) = 1.898(3); B(1)–N(1)–B(2) = 119.7(2), N(1)–B(1)–C(11) = 124.1(3), N(1)–B(1)–Br(1) = 118.0(2), C(11)–B(1)–Br(1) = 117.9(2), N(1)–B(2)–C(21) = 123.7(3), N(1)–B(2)–Br(2) = 118.9(2), C(21)–B(2)–Br(2) = 117.3(2); B(1)–N(1)–C(31)–C(32) = 62.7(4), B(2)–N(1)–C(31)–C(32) = −119.8(3); C(11)–C(15)//C(21)–C(25) = 10.5.

Table 1
Crystal data and structure refinement details for compounds **3**–**8** and **13**

	3	**4**	**5**	**6**	**7**	**8**	**13**
Formula	$C_{19}H_{22}BBr_2FeNSi$	$C_{17}H_{27}BBrFeNSi$	$C_{23}H_{27}B_2Br_2Fe_2NSi$	$C_{41}H_{41}B_2Fe_2N_3O_3$	$C_{78}H_{75}B_3Fe_3N_3O_3$	$C_{52}H_{61}B_4Br_2Fe_4N_3Si_2$	$C_{16}H_{12}B_2Br_3FeN$
Formula weight	518.95	420.06	638.69	757.09	1302.39	1210.68	535.47
Color, shape	Orange, block	Red–brown, plate	Red–brown, block	Orange, plate	Brown, rod	Brown, rod	Orange, block
Temperature (K)	147(2)	173(2)	173(2)	145(2)	222(2)	142(2)	144(2)
Radiation (Å)	Mo–K_α, 0.71073	Mo–K_α, 0.71073	Mo–K_α, 0.71073	Mo–K_α, 0.71073	Mo–K_α, 0.71073	Mo–K_α, 0.71073	Mo–K_α, 0.71073
Crystal system	Monoclinic	Orthorhombic	Monoclinic	Monoclinic	Triclinic	Monoclinic	Monoclinic
Space group	$P2_1/c$	$Pna2_1$	$P2_1/n$	$P2_1/c$	$P\bar{1}$	$P2_1/n$	Cc
a (Å)	9.0187(19)	26.973(2)	16.238(4)	23.940(5)	10.420(2)	11.9419(18)	7.0854(8)
b (Å)	23.362(3)	6.4529(5)	9.529(2)	7.9246(9)	14.198(3)	25.606(3)	17.975(3)
c (Å)	9.9892(12)	10.9733(6)	17.181(4)	20.198(2)	24.874(5)	17.086(4)	13.557(3)
α (°)	90	90	90	90	103.913(15)	90	90
β (°)	100.802(15)	90	111.910(10)	111.429(9)	93.960(16)	95.508 (14)	100.001 (15)
γ (°)	90	90	90	90	110.28(3)	90	90
V (Å^3)	2067.4(6)	1909.9(2)	2466.4(10)	3567.1(9)	3303.4(12)	5200.5(15)	1700.4(5)
Z	4	4	4	4	2	4	4
D_{calc} (g cm^{-3})	1.667	1.461	1.720	1.410	1.309	1.546	2.092
μ (mm^{-1})	4.655	2.940	4.477	0.857	0.702	2.715	7.931
Crystal size (mm)	0.55 × 0.38 × 0.33	0.41 × 0.28 × 0.12	0.20 × 0.20 × 0.10	0.40 × 0.26 × 0.06	0.80 × 0.33 × 0.10	0.34 × 0.15 × 0.06	0.70 × 0.28 × 0.20
Reflections collected	37 738	29 224	23 622	73 233	40 776	113 671	15 722
Reflections observed [$I > 2\sigma(I)$]	4841	3519	3229	5958	7376	7733	4319
Independent reflections	6334	3894	4524	12 043	16 172	13 633	5162
R_{int}	0.0366	0.0701	0.0661	0.1217	0.1063	0.1637	0.0367
T_{min}/T_{max}	0.134/0.215	0.379/0.719	0.468/0.663	0.864/0.950	0.691/0.932	0.503/0.859	0.084/0.205
Data/restraints/parameters	6334/0/281	3894/1/199	4524/0/280	12 043/0/464	16 172/0/814	13 633/6/604	5162/2/208
R_1, wR_2 [$I > 2\sigma(I)$]	0.0343, 0.0716	0.0467, 0.1025	0.0452, 0.0756	0.0606, 0.0887	0.0636, 0.1313	0.0679, 0.1176	0.0284, 0.0529
R_1, wR_2 (all data)	0.0581, 0.0783	0.0659, 0.1092	0.0674, 0.0817	0.1668, 0.1119	0.1681, 0.1674	0.1582, 0.1460	0.0434, 0.0580
Goodness-of-fit	1.123	1.068	1.117	1.016	0.925	1.140	0.849
Largest difference peak and hole (e Å^{-3})	0.456, −0.532	2.322, −0.605	0.429, −0.625	0.586, −0.479	0.757, −0.520	1.013, −0.913	0.550, −0.532

tions described above for **3** and **5**. According to the torsion angles N(1)–B(1)–N(2)–B(2) and B(1)–N(2)–B(2)–N(3) of 147.3(2) and 150.3(2)°, respectively, the three nitrogen atoms and the two boron atoms are not located in the same plane. Interestingly, the N–B–N–B–N backbone exhibits a 'W' shape in the solid state with all three 4-methoxyphenyl substituents pointing towards the same side of the molecule.

The X-ray crystal structure analysis of **7** ($P\bar{1}$; Fig. 5) reveals a trinuclear aggregate with a borazine core rather than a diazadiboretidine derivative. All six B–N bond lengths are equal within experimental error and possess an average value of 1.455(5) Å close to those found for the internal B–N bonds in **6**. Similar to 1,3,5-triferrocenylbenzene [19], the ferrocenyl substituents in **7** adopt an up-up-down conformation with respect to the central six-membered ring. This is in striking contrast to the up-up-up conformation of parent ferrocenylborazine **2** and ferrocenylboroxine **9** in the solid state [14]. In order to reduce the steric strain of **7**, the 4-methoxyphenyl rings are turned into an orthogonal position with respect to the mean plane of the borazine heterocycle [torsion angles: B(1)–N(1)–C(31)–C(32) = −61.4(4), B(2)–N(2)–C(61)–C(62) = 78.0(4), B(3)–N(3)–C(91)–C(92) = −93.5(4)°]. The B_3N_3 fragment is distorted from an ideal planar structure and exhibits a puckered chair-conformation [e.g. torsion angle: N(1)–B(1)–N(3)–B(3) = 20.0(5)°].

The B_4N_3 backbone of the tetranuclear open-chain species **8** ($P2_1/n$; Fig. 6) adopts a chiral helical conformation in the crystal lattice. According to its centrosymmetric space group $P2_1/n$, the crystal consists of a racemic mixture of left- and right-handed helices. Even though a trimethylsilyl group on N(1) [N(3)] is located in proximity to a bromo substituent on B(4) [B(1)], ring closure with elimination of trimethylsilyl bromide did obviously not occur [Si(1)···Br(2) = 4.85; Si(2)···Br(1) = 5.00 Å]. To test, whether the center of the molecule indeed contains an N–H group, or whether it might rather be an O atom, both models were refined. From the *R*-values alone, a distinction may not be conclusive (GOF = 1.140 for N–H and 1.149 for O). A comparison of the refined values of the thermal parameters, however, especially the rigid bond test described by Hirshfeld [20], confirmed the presence of an N–H group. Moreover, the hydrogen atom attached to N(2) was clearly visible in the difference Fourier synthesis, even when the refinement was performed with oxygen instead of nitrogen. The terminal B–N bonds are short [B(1)–N(1) = 1.408(6), B(4)–N(3) = 1.411(6) Å] and possess a planar conformation [C(11)–B(1)–N(1)–B(2) = 1.4(7), C(71)–B(4)–N(3)–B(3) = 9.0(7)°], which is indicative for some degree of double bond character (cf. the B–N bond in the mononuclear complex **3**). In contrast, the adjacent bonds B(2)–N(1) and B(3)–N(3) are not only longer [1.495(6) and 1.473(6) Å, respectively] but also substantially twisted [B(1)–N(1)–B(2)–C(31) = −113.9(5), B(4)–N(3)–B(3)–C(51) = −118.3(5)°] and can thus be regarded as single bonds. The central boron–nitrogen bonds possess intermediate values of B(2)–N(2) = 1.421(6) and B(3)–N(2) = 1.443(6) Å and torsion angles of B(3)–N(2)–B(2)–C(31) = −168.7(5) and B(2)–N(2)–B(3)–C(51) = −157.7(5)° (cf. the B–N bonds of the dinuclear complex **5**). It can thus be concluded, that the electron lone pair of N(1) [N(3)] is delocalized almost exclusively into the p-orbital of B(1) [B(4)], while N(2) acts as a π-donor both towards B(2) and B(3), thereby forming a delocalized system which is isoelectronic to the allyl cation.

In the BNB-bridged *ansa*-ferrocene **13** (*Cc*; Fig. 7), both B–N bond lengths possess values almost identical to those found in the corresponding open-chain diborylamine **5** [**13**: B(1)–N(1) = 1.448(5), B(2)–N(1) = 1.431(4) Å; **5**: B(1)–N(1) = 1.426(6) and B(2)–N(1) = 1.447(6) Å]. Moreover, the BNB bond angle of **13** [B(1)–N(1)–B(2) = 119.7(2)°] does not deviate significantly from the ideal angle of 120° expected for a planar sp^2-hybridized nitrogen atom. The cyclopentadienyl rings of the ferrocene backbone are only slightly tilted (dihedral angle between planes C(11)–C(15)//C(21)–C(25) = 10.5°), indicating, that the *ansa*-bridge does not cause any substantial strain in the molecule. To meet the requirements of the rather long B(1)–N(1)–B(2) linker, the ferrocene moiety deviates from an eclipsed conformation (torsion angle B(1)–COG(1)–COG(2)–B(2) = 30.8°; COG: center of gravity of the respective cyclopentadienyl ring). As a result, each of the four protons of the cyclopentadienyl rings is placed in its own unique chemical environment. The fact, that only two proton resonances are visible in the ^{1}H-NMR spectrum of **13** can be explained by a dynamic behavior of the molecule (mutual twisting of the cyclopentadienyl rings), which is fast on the NMR time scale and leads to a higher average symmetry of **13** in solution. The torsion angle B(1)–N(1)–C(31)–C(32) of 62.7(4)° indicates a low degree of N-phenyl back bonding in the solid state. The nitrogen atom thus acts as a π-donor mainly towards the boron atoms.

2.4. Electrochemical measurements

All B–N bridged species described here have been investigated using cyclic voltammetry. In most cases, ferrocene oxidation was accompanied by irreversible degradation processes, thereby rendering impossible any more detailed investigation of the magnetic and/or electronic properties of the aimed-for mixed-valence species.

3. Conclusion

Mono- to tetranuclear ferrocene aggregates are readily accessible via the stepwise assembly of boron–nitrogen bonds. The most stable compound consists of a central borazine skeleton with three pendent ferrocenyl moieties grouped around it. It has not yet been possible to force the system towards the formation of 1,3,2,4-diazadiboretidine heterocycles, even though sterically demanding nitrogen substituents (phenyl, *tert*-butyl, trimethylsilyl) were employed. Under thermodynamic control, aminolysis of boron halides usually leads to borazine formation. Nevertheless, the open-chain compound **8** could be isolated, which features a helical B_4N_3 backbone. In this special case, addition of a fourth boron atom to the growing B_3N_3 chain was able to compete successfully with the ring closure reaction.

Attempts to synthesize poly(ferrocenylenes) via the aminolysis of 1,1′-diborylated ferrocene building blocks were not met with success. In all cases, 1,3-dibora-[3]ferrocenophanes were obtained instead. These results indicate a strong preference for the formation of *intra*molecular BNB *ansa*-bridges over *inter*molecular BNB crosslinks. Even the borazine derivative **7**, which possesses 4-methoxyphenyl substituents at nitrogen in addition to the bulky ferrocenyl groups at boron, is still prone to hydrolysis. As expected, this problem is much worse in the case of the open-chain species. According to cyclic voltammetric measurements, oxidation of the ferrocene substituents was generally irreversible and led to the liberation of ferrocene. The degree of electronic communication via the B–N bonds in our compounds is therefore still unknown.

4. Experimental

4.1. General considerations

All reactions and manipulations of air-sensitive compounds were carried out in dry, oxygen-free Ar using standard Schlenk ware. Solvents were freshly distilled under N_2 from Na-benzophenone ($C_6H_5CH_3$, C_6H_{14}, C_7H_{16}) or stored over 4 Å molecular sieves prior to use (C_6D_6). NMR: JEOL JMN-GX 400, Bruker AMX 250, Bruker DPX 250 spectrometers. ^{11}B-NMR spectra are reported relative to external $BF_3 \cdot Et_2O$. Unless stated otherwise, all NMR spectra were run at ambient temperature. Abbreviations: s = singlet; d = doublet; t = triplet; vtr = virtual triplet; dd = doublet of doublets; br = broad; n.r. = multiplet expected in the ^{1}H-NMR spectrum but not resolved; n.o. = signal not observed; Me = methyl; Ph = phenyl; resonances marked with '*' belong to the central 4-methoxyphenyl group of **6**. Elemental analyses: Microanalytical laboratory of the J.W. Goethe-University Frankfurt (Main). $FcBBr_2$ (**1**) and 1,1′-fc$(BBr_2)_2$ (**10**) were prepared according to published procedures [17,21].

4.2. Preparation of *2*

Hexamethyldisilazane (0.89 g, 5.51 mmol) in $C_6H_5CH_3$ (10 ml) was added with stirring at 0 °C to a solution of **1** (1.96 g, 5.51 mmol) in $C_6H_5CH_3$ (30 ml). The reaction mixture was allowed to warm to ambient temperature and then stirred at 50 °C for 0.5 h, whereupon its color gradually changed from deep red to orange. After cooling to ambient temperature, the volume of the solution was reduced to about 15 ml in vacuo and the remaining liquid stored at −30 °C overnight. Compound **2** was obtained as orange crystalline solid, which was isolated by filtration and dried in vacuo. Yield: 1.02 g (88%). Slow evaporation of a C_6H_6 solution of **2** at ambient temperature yielded X-ray quality crystals.

^{11}B-NMR (128.4 MHz, $CDCl_3$): δ 34.7 ($h_{1/2} = 700$ Hz). ^{1}H-NMR (250.1 MHz, $CDCl_3$): δ 4.16 (s, 15H, C_5H_5), 4.48 (br, 12H, C_5H_4), 5.07 (br, 3H, NH). ^{13}C-NMR (62.9 MHz, $CDCl_3$): 68.9 (C_5H_5), 71.7, 71.9 (C_5H_4), n.o. (C_5H_4-*ipso*). Anal. Calc. for $C_{30}H_{30}B_3Fe_3N_3$: C, 56.96; H, 4.78; N, 6.64. Found: C, 56.98; H, 4.80; N, 6.74%.

4.3. Preparation of *3*

4-Bromo-*N*,*N*-bis(trimethylsilyl)aniline (2.19 g, 6.92 mmol) in C_6H_{14} (20 ml) was added at ambient temperature to **1** (2.46 g, 6.92 mmol) in C_6H_{14} (40 ml). The resulting mixture was first stirred at ambient temperature for 5 h and then concentrated to a volume of about 15 ml in vacuo. The orange solid **3**, which precipitated upon storage of the solution at −30 °C for 72 h, was isolated by filtration, triturated with C_5H_{12} and dried in vacuo. Yield: 3.22 g (90%).

^{11}B-NMR (128.4 MHz, C_6D_6): δ 30.9 ($h_{1/2} = 600$ Hz). ^{29}Si{^{1}H}-NMR (49.7 MHz, C_6D_6): δ 13.11 (s, $SiMe_3$). ^{1}H-NMR (250.1 MHz, C_6D_6): δ 0.24 (s, 9H, $SiMe_3$), 3.66 (vtr, 2H, $^3J(H,H) = {}^4J(H,H) = 1.8$ Hz, C_5H_4), 3.96 (s, 5H, C_5H_5), 4.03 (vtr, 2H, $^3J(H,H) = {}^4J(H,H) = 1.8$ Hz, C_5H_4), 6.45, 7.15 (2 × dd, 2 × 2H, $^3J(H,H) = 8.6$ Hz, $^5J(H,H) = 1.9$ Hz, Ph). ^{13}C-NMR (62.9 MHz, C_6D_6): δ 2.8 ($SiMe_3$), 69.6 (C_5H_5), 73.7, 77.3 (C_5H_4), n.o. (C_5H_4-*ipso*), 119.4 (C–Br), 130.7, 132.3 (Ph-2,3,5,6), 146.7 (C–N).

4.4. Preparation of *4*

A clear colorless solution of lithium *N*-*tert*-butyltrimethylsilylamide (1.03 g, 6.80 mmol; prepared in situ from *N*-*tert*-butyl trimethylsilylamine and n-BuLi) in C_6H_{14} (30 ml) was added dropwise with stirring at 0 °C to a solution of **1** (2.42 g, 6.80 mmol) in $C_6H_5CH_3$ (30

ml). The resulting deep red mixture was allowed to warm to ambient temperature and stirred for 1 h, whereupon a pale yellow precipitate formed, which was removed by filtration. The filtrate was evaporated to a volume of about 20 ml in vacuo and stored at −30 °C for 72 h. Compound **4**, which precipitated as orange crystalline solid, was isolated by filtration, triturated with pentane (10 ml) and dried in vacuo. Yield: 2.56 g (90%).

^{11}B-NMR (128.4 MHz, C_6D_6): δ 45.7 ($h_{1/2} = 140$ Hz). ^{1}H-NMR (250.1 MHz, $CDCl_3$): δ 0.15 (s, 9H, $SiMe_3$), 1.62 (s, 9H, CMe_3), 4.19 (s, 5H, C_5H_5), 4.43, 4.52 (2 × vtr, 2 × 2H, $^3J(H,H) = {}^4J(H,H) = 1.8$ Hz, C_5H_4). ^{13}C-NMR (62.9 MHz, $CDCl_3$): δ 5.7 ($SiMe_3$), 33.0 (CMe_3), 56.8 (CMe_3), 69.5 (C_5H_5), 72.5, 75.0 (C_5H_4) n.o. (C_5H_4-*ipso*).

4.5. Preparation of **5**

Sodium bis(trimethylsilyl)amide (0.17 g, 0.93 mmol) in $C_6H_5CH_3$ was slowly added with stirring at −78 °C to a solution of **1** in C_7H_{16} (0.66 g, 1.85 mmol). After the mixture had been allowed to warm to ambient temperature, NaBr was removed by filtration. X-ray quality crystals of **5** grew from the filtrate at ambient temperature over a period of several days. Yield: 0.49 g (83%).

^{29}Si{^{1}H}-NMR (49.7 MHz, C_6D_6): δ 5.91 (s, $SiMe_3$). ^{1}H-NMR (250.1 MHz, C_6D_6): δ 0.26 (s, 9H, $SiMe_3$), 4.04 (s, 10H, C_5H_5), 4.24, 4.53 (2 × vtr, 2 × 4H, $^3J(H,H) = {}^4J(H,H) = 1.8$ Hz, C_5H_4). ^{13}C-NMR (62.9 MHz, C_6D_6): δ 5.7 ($SiMe_3$), 69.8 (C_5H_5), 74.6, 76.6 (C_5H_4), n.o. (C_5H_4-*ipso*).

4.6. Preparation of **6**

A mixture of 4-methoxyaniline (0.89 g, 7.23 mmol) and Et_3N (1.47 g, 14.53 mmol) in $C_6H_5CH_3$ (30 ml) was added dropwise with stirring at −78 °C to a solution of **1** (2.58 g, 7.25 mmol) in $C_6H_5CH_3$ (40 ml). The color of the reaction mixture changed gradually from red to yellow, and a pale yellow precipitate formed upon warming to ambient temperature. The resulting slurry was stirred at ambient temperature for 24 h. After filtration, the volume of the filtrate was reduced to about 20 ml in vacuo. Compound **6**, which crystallized as an orange solid upon storage of the $C_6H_5CH_3$ solution at −30 °C for 72 h, was isolated by filtration, triturated with C_5H_{12} (10 ml) and dried in vacuo. Yield: 1.40 g (77%). Orange X-ray quality crystals of **6** were obtained from its C_6H_6 solution at ambient temperature.

^{11}B-NMR (128.4 MHz, $CDCl_3$): δ 35.3 ($h_{1/2} = 1400$ Hz). ^{1}H-NMR (250.1 MHz, $CDCl_3$): δ 3.61 (s, 3H, OCH_3^*), 3.66 (s, 6H, OCH_3), 4.00 (vtr, 4H, $^3J(H,H) = {}^4J(H,H) = 1.8$ Hz, C_5H_4), 4.02 (s, 10H, C_5H_5), 4.10 (vtr, 4H, $^3J(H,H) = {}^4J(H,H) = 1.8$ Hz, C_5H_4), 5.30 (s, 2H, NH), 6.50 (dd, 2H, $^3J(H,H) = 8.8$ Hz, $^5J(H,H) = 2.2$ Hz, Ph*-2,6 or Ph*-3,5), 6.55, 6.67 (2 × dd, 2 × 4H, $^3J(H,H) = 8.9$ Hz, $^5J(H,H) = 2.3$ Hz, Ph-2,3,5,6), 6.82 (dd, 2H, $^3J(H,H) = 8.8$ Hz, $^5J(H,H) = 2.2$ Hz, Ph*-2,6 or Ph*-3,5). ^{13}C-NMR (62.9 MHz, $CDCl_3$): δ 55.3 (OCH_3^*), 55.4 (OCH_3), 68.3 (C_5H_5), 70.1, 73.6 (C_5H_4), n.o. (C_5H_4-*ipso*), 113.3 (Ph*-2,6 or Ph*-3,5) 113.5, 123.9 (Ph-2,3,5,6), 128.1 (Ph*-2,6 or Ph*-3,5), 136.4 (C–N), 140.9 (C*–N), 154.8 (C–O), 155.2 (C*–O). ESI-MS: *m/z* 757 [M^+]. Anal. Calc. for $C_{41}H_{41}B_2Fe_2N_3O_3 \times 0.4C_7H_8$: C, 66.26; H, 5.61; N, 5.29. Found: C, 66.10; H, 5.64; N, 5.25%.

4.7. Preparation of **7**

4.7.1. Method 1

Compound **1** (0.33 g, 0.93 mmol) in $C_6H_5CH_3$ (20 ml) was added with stirring at −78 °C to **6** (0.70 g, 0.92 mmol) and Et_3N (0.19 g, 1.88 ml) in $C_6H_5CH_3$ (40 ml). The mixture was allowed to warm to ambient temperature and then heated under reflux for 2 h, whereupon its color changed gradually from red to orange, and a pale yellow precipitate formed. After filtration, the volume of the filtrate was reduced to about 10 ml. Compound **7**, which crystallized as orange solid upon storage of the filtrate at −30 °C for 12 h, was isolated by filtration, triturated with C_5H_{12} (5 ml) and dried in vacuo. Yield: 0.60 g (69%). Orange X-ray quality crystals of **7** were obtained from its C_6H_6 solution at ambient temperature.

4.7.2. Method 2

Compound **6** (0.75 g, 0.99 mmol) in $C_6H_5CH_3$ (30 ml) was treated with n-BuLi (0.13 g, 2.03 mmol) in C_6H_{14} (1.2 ml) and stirred for 0.5 h at −78 °C. **1** (0.35 g, 0.98 mmol) in $C_6H_5CH_3$ (20 ml) was added at −78 °C, the orange slurry was allowed to warm to ambient temperature and stirred for 2 h. After filtration, the volume of the filtrate was reduced to about 10 ml. Compound **7**, which was obtained as an orange crystalline solid upon storage of the solution at −30 °C for 12 h, was isolated by filtration, triturated with C_5H_{12} (5 ml) and dried in vacuo.Yield: 0.68 g (73%).

^{11}B-NMR (128.4 MHz, $CDCl_3$): δ 35.1 ($h_{1/2} = 1700$ Hz). ^{1}H-NMR (250.1 MHz, $CDCl_3$): δ 2.87 (vtr, 6H, $^3J(H,H) = {}^4J(H,H) = 1.8$ Hz, C_5H_4), 3.90 (s, 9H, OCH_3), 4.00 (vtr, 6H, $^3J(H,H) = {}^4J(H,H) = 1.8$ Hz, C_5H_4), 4.06 (s, 15H, C_5H_5), 6.90, 7.21 (2 × dd, $^3J(H,H) = 8.8$ Hz, $^5J(H,H) = 2.3$ Hz, 2 × 6H, Ph-2,3,5,6). ^{13}C-NMR (62.9 MHz, $CDCl_3$): δ 55.4 (OCH_3), 68.6 (C_5H_5), 70.2, 77.0 (C_5H_4), n.o. (C_5H_4-*ipso*), 113.1, 131.6 (Ph-2,3,4,5), 141.1 (C–N), 157.3 (C–O). ESI-MS: *m/z* 951 [M^+]. Anal. Calc. for $C_{51}H_{48}B_3Fe_3N_3O_3$: C, 64.42; H, 5.09; N, 4.42. Found: C, 64.29; H, 5.47; N, 4.47%.

4.8. Preparation of **8**

Sodium bis(trimethylsilyl)amide (0.11 g, 0.60 mmol) in $C_6H_5CH_3$ (1 ml) was filled into an NMR tube and evaporated to dryness in vacuo. Solid **1** (0.21 g, 0.59 mmol) was added and the mixture treated with 1 ml of C_6D_6. Few X-ray quality crystals were obtained upon storage of the solution at ambient temperature over a period of several days.

4.9. Preparation of **9**

Compound **6** (0.27 g, 0.36 mmol) was dissolved in $C_6H_5CH_3$ (15 ml, commercially available $C_6H_5CH_3$ was used as purchased without drying; no additional water was required) and exposed to air over a period of 10 days. The color of the solution gradually changed from yellow to brown, and yellow X-ray quality crystals grew from the mother liquor. Yield: 0.13 g (85%). Note: Compound **9** has also been obtained in comparable yield via the controlled hydrolysis of **7**.

^{11}B-NMR (128.4 MHz, $CDCl_3$): δ 31.4 ($h_{1/2} = 320$ Hz). ^{1}H-NMR (250.1 MHz, $CDCl_3$): δ 4.19 (s, 15H, C_5H_5), 4.56, 4.69 ($2 \times$ n.r., 2×6H, C_5H_4). ^{13}C-NMR (62.9 MHz, $CDCl_3$): δ 68.8 (C_5H_5), 73.1, 74.3 (C_5H_4), n.o. (C_5H_4-*ipso*). ESI-MS: *m*/*z* 635.5 [M^+]. Anal. Calc. for $C_{30}H_{27}B_3Fe_3O_3$: C, 56.70; H, 4.28. Found: C, 56.42; H, 4.57%.

4.10. Preparation of **11**

4-Bromo-*N*,*N*-bis(trimethylsilyl)aniline (0.61 g, 1.93 mmol) in $C_6H_5CH_3$ (40 ml) was added with stirring to **10** (1.02 g, 1.94 mmol) in $C_6H_5CH_3$ (120 ml) at -78 °C. The reaction mixture was allowed to warm to ambient temperature and stirred for 4 h whereupon the color changed gradually from yellow to red. The solution was evaporated in vacuo until a red oil remained, which was subsequently triturated with C_6H_{14} (2×30 ml) for further purification. Yield: 0.98 g (73%).

^{11}B-NMR (128.4 MHz, C_6D_6): δ 37 (shoulder), 41.9 ($h_{1/2} = 350$ Hz). ^{29}Si{^{1}H}-NMR (49.7 MHz, C_6D_6): δ 9.44 (s, $SiMe_3$). ^{1}H-NMR (250.1 MHz, C_6D_6): δ 0.19 (s, 9H, $SiMe_3$), 3.68, 3.97, 4.37, 4.49 ($4 \times$ vtr, 4×2H, $^3J(H,H) = {}^4J(H,H) = 1.8$ Hz, C_5H_4), 6.37, 7.11 ($2 \times$ dd, 2×2H, $^3J(H,H) = 8.5$ Hz, $^5J(H,H) = 1.9$ Hz, Ph-2,3,5,6). ^{13}C-NMR (62.9 MHz, C_6D_6): δ 2.5 ($SiMe_3$), 76.5, 78.4, 79.4, 79.7 (C_5H_4), n.o. (C_5H_4-*ipso*), 119.7 (C–Br), 130.6, 132.4 (Ph-2,3,5,6), 146.1 (C–N).

4.11. Preparation of **12**

Compound **10** (0.48 g, 0.91 mmol) in $C_6H_5CH_3$ (10 ml) was added dropwise with stirring at ambient temperature to 4-bromo-*N*,*N*-bis(trimethylsilyl)aniline (0.58 g, 1.83 mmol) in $C_6H_5CH_3$ (40 ml). The color of the reaction mixture gradually changed from red to yellow. After the solution had been stirred for 5 h at ambient temperature, its volume was reduced to about 15 ml in vacuo. Compound **12**, which crystallized as orange solid upon storage of the solution at -30 °C for 12 h, was isolated by filtration, triturated with C_5H_{12} (2×5 ml) and dried in vacuo. Yield: 0.73 g (94%).

^{11}B-NMR (128.4 MHz, $CDCl_3$): δ 32.5 ($h_{1/2} = 1200$ Hz). ^{29}Si{^{1}H}-NMR (49.7 MHz, $CDCl_3$): δ 14.48. ^{1}H-NMR (250.1 MHz, $CDCl_3$): δ 0.21 (s, 18H, $SiMe_3$), 3.49, 4.13 ($2 \times$ vtr, $^3J(H,H) = {}^4J(H,H) = 1.9$ Hz, 2×4H, C_5H_4), 6.77, 7.40 ($2 \times$ dd, $^3J(H,H) = 6.5$ Hz, $^5J(H,H) = 2.0$ Hz, 2×4H, Ph-2,3,5,6). ^{13}C-NMR (62.9 MHz, $CDCl_3$): δ 2.4 ($SiMe_3$), 74.6, 77.4 (C_5H_4), n.o. (C_5H_4-*ipso*), 119.0 (C–Br), 130.1, 132.0 (Ph-2,3,5,6), 146.2 (C–N).

4.12. Preparation of **13**

4.12.1. Method 1

Compound **11** (0.67 g, 0.97 mmol) in $C_6H_5CH_3$ (120 ml) was heated under reflux for 2.5 h. The solution was concentrated to a volume of about 30 ml in vacuo and stored at -30 °C overnight. After filtration from a small amount of yellow precipitate, the filtrate was further concentrated to a volume of 10 ml. Compound **13**, which crystallized as orange solid upon storage of the filtrate at -30 °C for 12 h, was isolated by filtration, triturated with C_5H_{12} (5 ml) and dried in vacuo. Yield: 0.40 g (77%). Yellow X-ray quality crystals of **13** were grown from $C_6H_5CH_3$ at -30 °C.

4.12.2. Method 2

Compound **12** (1.20 g, 1.41 mmol) in $C_6H_5CH_3$ (40 ml) was added with stirring to **10** (0.74 g, 1.41 mmol) in $C_6H_5CH_3$ (40 ml) at -78 °C. The reaction mixture was allowed to warm to ambient temperature and heated under reflux for 2.5 h whereupon its color changed gradually from yellow to red. The solution was cooled to ambient temperature and evaporated slowly in vacuo to yield red crystals of **13**. Yield: 1.38 g (91%).

^{11}B-NMR (128.4 MHz, $CDCl_3$): δ 40.0 ($h_{1/2} = 650$ Hz). ^{1}H-NMR (250.1 MHz, $CDCl_3$): δ 4.32, 4.60 ($2 \times$ vtr, 2×4H, $^3J(H,H) = {}^4J(H,H) = 1.6$ Hz, C_5H_4), 6.98, 7.46 ($2 \times$ d, 2×2H, $^3J(H,H) = 8.5$ Hz, Ph-2,3,5,6). ^{13}C-NMR (62.9 MHz, $CDCl_3$): δ 77.2, 78.4 (C_5H_4), n.o. (C_5H_4-*ipso*), 120.1 (C–Br), 130.1, 132.0 (Ph-2,3,5,6), 145.0 (C–N).

4.13. X-ray crystal structure determination of **3**–**8** and **13**

The data collections for **3**–**8** and **13** were performed on a SIEMENS-SMART-CCD-three-circle-diffractometer. The structures were solved with direct methods using the program SIR-92 [22] for **6** and SHELXS [23] for all the other structures. The structures were refined on

F^2 values using the program SHELXL-97 [24]. Absorption corrections were performed with the program SADABS [25]. Except of **3**, all non-hydrogen atoms were refined anisotropically, whereas the hydrogen atoms were treated using a riding model. In the case of **3**, the hydrogen atoms of the methyl groups were placed at geometrically optimized positions and treated as riding atoms; the remaining hydrogen atoms were taken from a difference Fourier synthesis and refined with isotropic thermal parameters. The high residual electron density in **4** is possibly due to absorption effects. There is just one peak with more than 1 electron per $Å^3$ in the final difference electron density map and this peak is very close (1.39 Å) to the bromine atom. The asymmetric unit of **7** contains 4.5 C_6H_6 solvent molecules. In **8**, the asymmetric unit contains a solvate molecule identified as C_6H_6, which is disordered. Its C–C bond lengths were constrained to 1.38(3) Å. The largest residual electron density is found at this disordered C_6H_6 molecule. Further details of the structure analyses are compiled in Table 1.

5. Supplementary material

Crystallographic data for the structure analysis have been deposited with the Cambridge Crystallographic Data Centre, CCDC no. 188759–188765 for compounds **3**, **4**, **5**, **6**, **7**, **8** and **13**, respectively. Copies of this information may be obtained free of charge from The Director, CCDC, 12 Union Road, Cambridge CB2 1EZ, UK (Fax: +44-1223-336033; e-mail: deposit@ccdc.cam.ac.uk or www: http://www.ccdc.cam.ac.uk).

Acknowledgements

This work was generously supported by the *Deutsche Forschungsgemeinschaft* (DFG).

References

[1] P. Nguyen, P. Gómez-Elipe, I. Manners, Chem. Rev. 99 (1999) 1515.
[2] D.W. Bruce, D. O'Hare (Eds.), Inorganic Materials, John Wiley & Sons, Chichester, UK, 1992.
[3] N.J. Long, Angew. Chem. Int. Ed. Engl. 34 (1995) 21.
[4] L. Oriol, J.L. Serrano, Adv. Mater. 7 (1995) 348.
[5] A. Togni, T. Hayashi (Eds.), Ferrocenes, VCH, Weinheim, 1995.
[6] M. Iyoda, T. Kondo, T. Okabe, H. Matsuyama, S. Sasaki, Y. Kuwatani, Chem. Lett. (1997) 35.
[7] B. Chiavarino, M.E. Crestoni, A.D. Marzio, S. Fornarini, M. Rosi, J. Am. Chem. Soc. 121 (1999) 11204.
[8] R.J. Boyd, S.C. Choi, C.C. Hale, Chem. Phys. Lett. 112 (1984) 136.
[9] G. Heller, A. Meller, in: K. Niedenzu, K.-C. Buschbeck (Eds.), Gmelin Handbook of Inorganic Chemistry, new supplementary series volume 44/13, Springer-Verlag, Berlin, Heidelberg, New York, 1977.
[10] A. Meller, in: K. Niedenzu (Ed.), Gmelin Handbook of Inorganic Chemistry, new supplementary series volume 51/17, Springer-Verlag, Berlin, Heidelberg, New York, 1977.
[11] A.F. Holleman, N. Wiberg, Lehrbuch der Anorganischen Chemie, de Gruyter, Berlin, New York, 1995.
[12] S. Guo, F. Peters, F.F. de Biani, J.W. Bats, E. Herdtweck, P. Zanello, M. Wagner, Inorg. Chem. 40 (2001) 4928.
[13] J.C. Kotz, W.J. Painter, J. Organomet. Chem. 32 (1971) 231.
[14] J.W. Bats, K. Ma, M. Wagner, Acta Crystallogr. Sect. C 58 (2002) m129.
[15] M. Herberhold, U. Dörfler, W. Milius, B. Wrackmeyer, J. Organomet. Chem. 492 (1995) 59.
[16] H. Nöth, B. Wrackmeyer, Nuclear Magnetic Resonance Spectroscopy of Boron Compounds, Springer, Berlin, 1978.
[17] W. Ruf, T. Renk, W. Siebert, Z. Naturforsch. Teil. B 31 (1976) 1028.
[18] F. Jäkle, T. Priermeier, M. Wagner, Organometallics 15 (1996) 2033.
[19] P. Stepnicka, I. Cisarova, J. Sedlacek, J. Vohlidal, M. Polasek, Collect. Czech. Chem. Commun. 62 (1997) 157.
[20] F.L. Hirshfeld, Acta Crystallogr. Sect. A 32 (1976) 239.
[21] T. Renk, W. Ruf, W. Siebert, J. Organomet. Chem. 120 (1976) 1.
[22] A. Altomare, G. Cascarano, C. Giacovazzo, A. Guagliardi, M.C. Burla, G. Polidori, M. Camalli, J. Appl. Crystallogr. 27 (1994) 435.
[23] G.M. Sheldrick, Acta Crystallogr. Sect. A 46 (1990) 467.
[24] G.M. Sheldrick, SHELXL-97, Program for the Refinement of Crystal Structures, University of Göttingen, Göttingen, Germany, 1997.
[25] G.M. Sheldrick, SADABS, Program for the Absorption Correction of Area Detector Data, University of Göttingen, Göttingen, Germany, 1996.